

Children's Mercy Kansas City

**SHARE @ Children's Mercy**

---

Manuscripts, Articles, Book Chapters and Other Papers

---

7-2023

## **A whole-joint histopathologic grading system for murine knee osteoarthritis.**

Caleb W. Grote

Matthew J. Mackay

Qinghua Lu

Xiangliang Liu

Anders R. Meyer

*See next page for additional authors*

Let us know how access to this publication benefits you

Follow this and additional works at: <https://scholarlyexchange.childrensmercy.org/papers>

---

---

**Creator(s)**

Caleb W. Grote, Matthew J. Mackay, Qinghua Lu, Xiangliang Liu, Anders R. Meyer, and Jinxi Wang

## RESEARCH ARTICLE

# A whole-joint histopathologic grading system for murine knee osteoarthritis

Caleb W. Grote<sup>1,2</sup> | Matthew J. Mackay<sup>1</sup> | Qinghua Lu<sup>1</sup> | Xiangliang Liu<sup>1</sup> |  
Anders R. Meyer<sup>3</sup> | Jinxi Wang<sup>1,4</sup> 

<sup>1</sup>Harrington Laboratory for Molecular Orthopedics, Department of Orthopedic Surgery, University of Kansas Medical Center, Kansas City, Kansas, USA

<sup>2</sup>Department of Orthopedics and Musculoskeletal Sciences, Children's Mercy Hospitals & Clinics, Kansas City, Missouri, USA

<sup>3</sup>Department of Pathology and Laboratory Medicine, University of Kansas Medical Center, Kansas City, Kansas, USA

<sup>4</sup>Department of Biochemistry & Molecular Biology, University of Kansas Medical Center, Kansas City, Kansas, USA

## Correspondence

Jinxi Wang, Department of Orthopedic Surgery, University of Kansas Medical Center, 3901 Rainbow Blvd, MS #3017, Kansas City, KS 66160, USA.  
Email: [jwang@kumc.edu](mailto:jwang@kumc.edu)

## Funding information

National Institute of Arthritis and Musculoskeletal and Skin Diseases, Grant/Award Number: R01 AR059088

## Abstract

This study aims to develop a comprehensive and easily executable histopathologic grading scheme for murine knee osteoarthritis (OA) using specific scoring criteria for both cartilage and periarticular changes, which may overcome important limitations of the existing grading systems. The new grading scheme was developed based on mouse knee OA models with observation periods up to 24 months of age (spontaneous OA) or 24-week post-injury (posttraumatic OA). Semi-quantitative assessments of the histopathologic OA changes were applied to all four quadrants per femorotibial joint for 50 joints (200 quadrants) using specific scoring criteria rather than mild to severe grades. Scoring elements per quadrant were as follows: cartilage lesion (0–7), osteophyte (0–3), subchondral bone change (0–3), synovitis (0–3), and ectopic periarticular soft-tissue chondrogenesis and ossification (0–3). The new histopathologic grading scheme had high intra- and interobserver reproducibility (correlation coefficients  $r > 0.95$ ) across experienced and novice observers. Sensitivity and reliability analyses confirmed the ability of the new scheme to detect minimal but significant OA progression ( $p < 0.01$ ) within a 2-week interval and to accurately identify tissue- and quadrant-specific OA severity within the joints. In conclusion, this study presents the first whole-joint histopathologic grading scheme for murine knee OA that covers all-stage osteoarthritic changes in all major joint tissues, including periarticular soft-tissue ossification that is not included in any of the existing OA grading systems. This reproducible scheme is easy to execute and sensitive to minimal OA progression without using computer software, suitable for quick OA severity assessments of the entire femorotibial joint.

## KEYWORDS

animal model, histologic grading, histopathology, mouse osteoarthritis, osteoarthritis

This is an open access article under the terms of the Creative Commons Attribution-NonCommercial-NoDerivs License, which permits use and distribution in any medium, provided the original work is properly cited, the use is non-commercial and no modifications or adaptations are made.

© 2022 The Authors. *Journal of Orthopaedic Research*© published by Wiley Periodicals LLC on behalf of Orthopaedic Research Society.

## 1 | INTRODUCTION

Osteoarthritis (OA) is one of the leading causes of chronic disability in the United States and has a significant socioeconomic burden accounting for \$185 billion dollars each year in medical care expenditures.<sup>1</sup> Reproducible and reliable histologic assessments of OA severity in animal models are critical for evaluating the efficacy of therapeutic agents designed to prevent or attenuate the disease and for comparing results among researchers using standardized grading criteria.<sup>2</sup>

Several semi-quantitative histologic OA grading systems have been created to assess OA severity in humans and animal models.<sup>3-11</sup> These systems have laid solid foundations with valuable methodologies for OA grading. Nevertheless, specific limitations remain to be addressed. For example, the most widely used histologic OA grading systems for humans and mice mainly focus on articular cartilage while scoring methods for periarticular tissues are either undefined or recommended with subjective scoring categories (e.g., mild, moderate, and severe),<sup>3-5,7</sup> though OA is considered a disease of both articular cartilage and the periarticular tissues.<sup>12,13</sup> A few grading systems have evaluated osteophytes, subchondral bone change, and synovitis by histomorphometry using computer software or micrometry<sup>9,10</sup>; those quantitative methods can improve the accuracy of measurements tailored to specific needs but may not be suitable for quick screening of numerous histologic images due to the time-consuming nature. Furthermore, some important osteoarthritic changes, such as ectopic chondrogenesis and ossification in the periarticular soft tissues are not included in any of the existing histologic OA grading systems.

The objective of this study was to develop a more comprehensive, easily executed, and highly reproducible histologic OA grading scheme with specific scoring elements covering articular cartilage and all periarticular changes seen in murine models of spontaneous and posttraumatic knee OA. The proposed new grading scheme focuses on mouse knee OA because mouse OA models remain the most popular due to relatively low cost, ease of breeding, modifiable genetics, and reproducible outcomes.<sup>14-16</sup>

The novel grading scheme reported here has added many new articular and periarticular OA grading elements, including late-stage cartilage and subchondral bone lesions as well as ectopic chondrogenesis and ossification in the periarticular soft tissues, that have not been encompassed in the existing grading systems.

## 2 | MATERIALS AND METHODS

### 2.1 | Murine models of osteoarthritis

The development of this histologic grading scheme was based on our OA histopathology experience with both spontaneous and posttraumatic knee OA models in mice. BALB/c background wild-type (WT) mice and *Nfat1*<sup>-/-</sup> mice that carry mutant NFAT1 (the nuclear factor of activated T cells-1) alleles and exhibit dysregulated immune responses<sup>17,18</sup> and spontaneous OA in the synovial joints,<sup>19-22</sup> both sexes, were utilized for the study of spontaneous OA. *Nfat1*<sup>-/-</sup> knees were evaluated from 2 to

24 months of age and WT knees were examined at 18 and 24 months of age.<sup>19-22</sup> Posttraumatic OA (PTOA) models that were induced in WT mice by surgical destabilization of the medial meniscus (DMM) or anterior cruciate ligament transection (ACL) as described by Glasson et al.<sup>23</sup> were examined at 2, 4, 8, 16, and 24 weeks post-surgery (unpublished results). All animal procedures were performed with the approval of the Institutional Animal Care and Use Committee in compliance with all federal and state laws and regulations.

### 2.2 | Preparation of tissue sections and histologic images

Mouse knee joint tissue samples were fixed in 2% paraformaldehyde, decalcified in 25% formic acid (Sigma-Aldrich, Cat. #F0507), embedded in paraffin (Thermo Fisher Scientific, Cat. #22900701), and sectioned coronally to examine both the medial and lateral compartments. Tissue sections at 5- $\mu$ m-thick were obtained every 70-80  $\mu$ m across the entire joint, with approximately 40 tissue slides per joint. Safranin-O and fast green stains were performed to identify cartilage cells and matrices within the joints. Hematoxylin-Eosin (H&E) stains were used to further examine the cellular and structural details. Histologic images were acquired with a ZEISS-Axioskop microscope equipped with a digital camera. General histopathologic analysis was conducted as described previously.<sup>19-22</sup>

### 2.3 | Literature review and justification for new OA scoring elements

A comprehensive review of published articles (PubMed, 1960-2021) on OA histopathology in humans and rodents was conducted. Our literature review suggested that although the published grading systems have included most histopathologic features of OA, some important osteoarthritic changes are either not specified or difficult to grade due to the complexities of methodology. Therefore, it is necessary to propose a novel knee OA grading scheme to cover additional osteoarthritic changes with simple and objective grading criteria. A brief comparison of the commonly cited grading systems and our newly developed grading scheme are summarized in Supporting Information: Table 1. This demonstrates that periarticular soft-tissue ossification is not included in any of the existing histopathologic OA grading systems and that no systems exist for organized "whole-joint" classification. Justifications for score ranges and elements of the new scheme as well as specific modifications to the existing grading systems are described below.

#### 2.3.1 | Weighting of score range for each joint tissue/OA change

While OA is now considered a whole-joint disease, breakdown of articular cartilage remains the most important hallmark of the disease; the articular cartilage that forms the articular surface is the most important component of the joint structure and has been

**TABLE 1** Whole-joint knee OA grading scheme

Category	Grade <sup>a</sup>	Histopathologic Change
Articular cartilage lesion	0	None
	0.5	Focal decrease/loss of Safranin-O or other proteoglycan staining without structural changes
	1	Focalized articular surface abrasion without loss of cartilage, with or without loss of proteoglycan staining
	1.5	Articular surface fibrillation within the superficial layer with discontinuity of cartilage surface lamina, with or without loss of proteoglycan staining
	2	Vertical clefts/cartilage loss down to the layer immediately below the superficial zone
	3	Vertical clefts/cartilage loss to the calcified cartilage extending <34% of the width of articular surface
	4	Vertical clefts/cartilage loss to the calcified cartilage extending 34%–67% of the width of articular surface
	5	Vertical clefts/cartilage loss to the calcified cartilage extending >67% of the width of articular surface
Chondro-osteophyte	6	Loss of both uncalcified and calcified cartilage with exposure of subchondral bone extending ≤50% of the width of articular surface
	7	Loss of both uncalcified and calcified cartilage with exposure of subchondral bone extending >50% of the width of articular surface
	0	None
	1	Chondrophyte (without ossification) in outer or inner joint margin
Subchondral bone change	2	Chondro-osteophyte (with ossification) in outer or inner joint margin
	3	Chondro-osteophyte in both inner and outer joint margins
	0	None
Synovitis	1	Focalized (≤50% of the width of articular surface) subchondral bone thickening (SCBT) <sup>b</sup> without bone cysts and sclerosis
	2	Extensive (>50% of the width of articular surface) SCBT without bone cysts and sclerosis, or focalized SCBT with bone cysts and/or sclerosis
	3	Extensive SCBT with bone cysts, sclerosis, microfracture, and/or chondrogenesis
	0	None
Ectopic ossification <sup>c</sup>	1	Focalized (≤50% of the lining surface of the synovium) synovial thickening <sup>b</sup>
	2	Extensive (>50% of the lining surface of the synovium) synovial thickening in either side plica or intercondylar notch/eminence
	3	Extensive synovial thickening in both side plica and intercondylar notch/eminence
	0	None
	1	Ectopic chondrogenic differentiation and chondrogenesis in synovium-capsule
	2	Ectopic chondrogenesis and ossification in synovium-capsule
	3	Ectopic chondrogenesis and ossification in synovium-capsule as well as ligament and/or muscle

<sup>a</sup>Grade number is set for each quadrant of the knee joint.

<sup>b</sup>Criterion of subchondral bone thickening or synovial thickening is set for >1.5-fold (visual estimate) over the same type of normal tissue at the same location.

<sup>c</sup>Ectopic ossification = Ectopic chondrogenesis and ossification in the periarticular soft tissues.

the focus of the existing OA grading systems for mice and humans.<sup>4,5,7</sup> In this study, therefore, we proposed a larger score range (0–7) per quadrant (medial femoral condyle/MFC, medial tibial plateau/LTP, lateral femoral condyle/LFC, or lateral tibial plateau/LTP) for cartilage lesions and a relatively smaller score range (0–3) per quadrant for osteophyte formation, subchondral bone change, synovitis, and ectopic soft-tissue ossification, respectively (Table 1).

### 2.3.2 | Articular cartilage lesion

Following the pioneering grading system reported in 1960 by Collins and McElligott,<sup>24</sup> the Mankin Grading System or Histochemical Grading System (HHGS) was published in 1971 for the evaluation of human hip OA<sup>3</sup> and has later been adapted to histologic evaluation of multiple animal models of OA,

including mice. Mankin grading focuses on cartilage changes including cartilage structure (0–6), chondrocyte cellularity (0–3), safranin-O staining (0–4), and tidemark integrity (0–1). However, concerns about the accuracy and reliability of the Mankin System for animal OA models have been raised, particularly for the thin cartilage of mice.<sup>25</sup> To address the concerns, the Osteoarthritis Research Society International (OARSI) working group published a new OA cartilage histopathology grading system in 2006,<sup>5</sup> which recommended grades 0–6 based on cartilage surface integrity, surface discontinuity, cartilage clefts/fissures, cartilage erosions, subchondral bone denudation, and deformation. This system was developed mainly for human OA pathology but has also been used for rodent OA. The OARSI histopathology initiative for mouse OA models was published in 2010, which recommended a semi-quantitative scoring system with grades 0–6 based mainly on the depth and percent of surface area of cartilage lesions.<sup>7</sup> In addition to those widely used histologic grading systems, other histologic OA grading systems have also been reported and utilized.<sup>6,8–10,26,27</sup>

Our cartilage scoring method was modified from the OARSI Initiative for assessments of OA in mice.<sup>7</sup> Based on the observations that osteoarthritic structural lesions were more prominent than proteoglycan staining and cellular changes in the thin cartilage of mouse knee OA models,<sup>7,19–22</sup> we proposed grades 0–7 per quadrant to primarily score the severity of structural changes in articular cartilage (Table 1). Our modifications included a new grade 1.5 to highlight the loss of surface lamina for the early phase of OA progression and a simplified scoring process by changing the criteria to <34%, 34%–67%, and >67% cartilage loss as opposed to

the OARSI Initiative grading with increments of 25%.<sup>7</sup> In addition, two new grades for lesions beyond the calcified cartilage layer were added to accommodate more severe cartilage lesions seen in late-stage OA in mice. The representative histologic images demonstrating our novel cartilage scoring elements are presented in Figure 1.

### 2.3.3 | Osteophyte formation

Currently, the osteophyte scoring method for murine knee OA recommended by the OARSI Initiative<sup>7</sup> is set 0 as normal, 1 = mild, 2 = moderate, and 3 = severe changes. Other osteophyte scoring methods have been recommended for rats<sup>9</sup> and guinea pigs<sup>8</sup> as part of the OARSI histopathology initiatives. Additional grading systems for osteophytes have been reported to score osteophyte size, maturity, and incidence.<sup>27–30</sup> The use of micro-CT for evaluation of osteophytes has also been reported with more detailed quantitative data.<sup>31</sup>

Osteophytes in the proposed new grading scheme are graded 0–3 for each quadrant of the knee joint based on the presence of chondrocytes or chondro-osteophytes at the inner and/or outer joint margins (Grade 0 = no osteophytes, Grade 1 = chondrocyte without ossification or osteophyte, Grade 2 = chondro-osteophyte or osteophyte at either inner or outer joint margin, Grade 3 = chondro-osteophyte or osteophyte at both inner and outer joint margins). This objectively highlights the progression of chondro-osteophyte formation and anatomic locations (Table 1 and Figure 2A). It also eliminates the need for measuring the size of osteophytes.

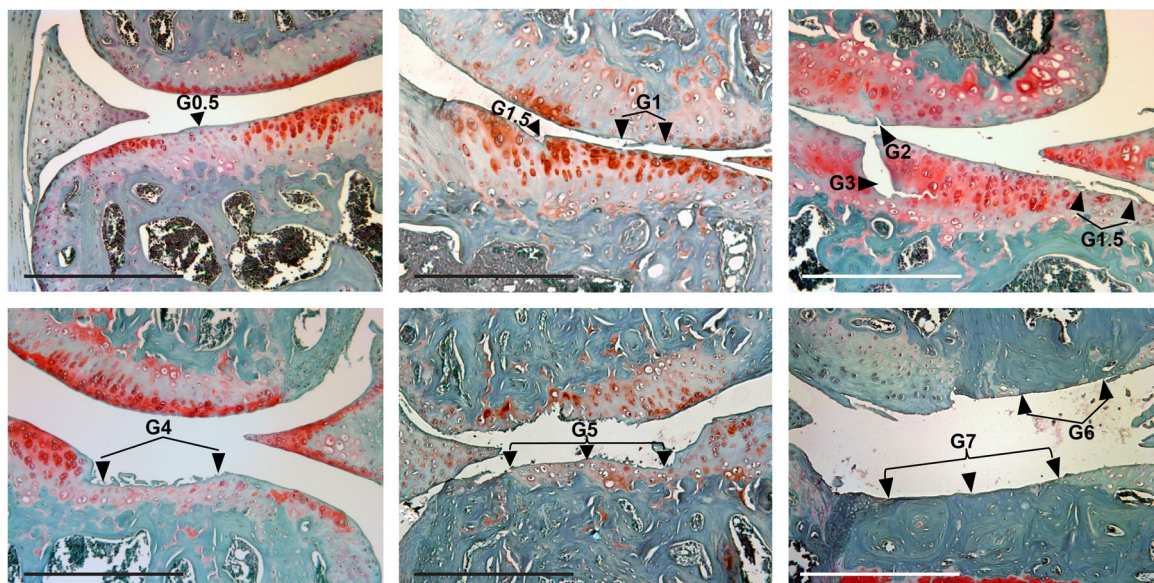


**FIGURE 1** Photomicrographs showing osteoarthritic cartilage lesions in the femoral condyle (upper portion) and tibia plateau (lower portion) of each micrograph. Cartilage proteoglycans are stained by safranin-O in red or pink at various intensities depending on the local pathologic changes. Arrowheads point to specific cartilage lesions with various OA cartilage grades as described in Table 1. OA, osteoarthritis. G0.5 = Cartilage grade 0.5, G1 = grade 1, G1.5 = grade 1.5, G2 = grade 2, G3 = grade 3, G4 = grade 4, G5 = grade 5, G6 = grade 6, and G7 = grade 7. Safranin-O and fast green stains, counterstained with hematoxylin. Scale bar = 100  $\mu$ m.

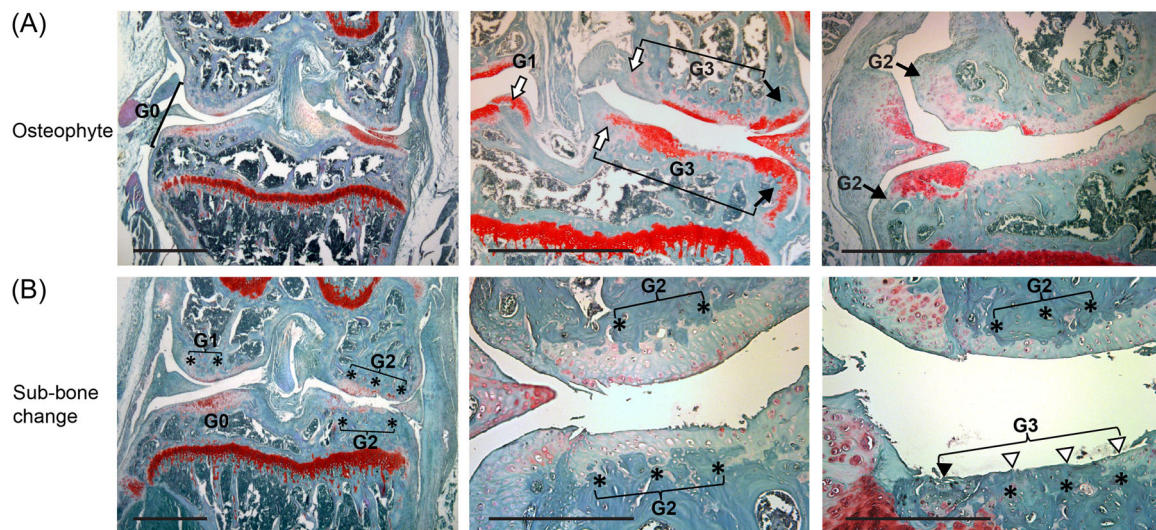


**FIGURE 2** (A) Photomicrographs showing chondro-osteophyte formation in the joint margin of the femoral condyle (upper portion) and tibial plateau (lower portion) of each graph. Black arrows point to chondro-osteophytes (both chondrogenesis and ossification with new bone marrow formation) in the outer joint margins; open arrows indicate chondrophytes in the inner joint margins. G0 = normal, G1 = grade 1, G2 = grade 2, G3 = grade 3. (B) Photomicrographs showing subchondral bone (sub-bone) changes in the femoral condyle (upper) and tibial plateau (lower). Areas with thickened subchondral bone are labeled with \*; black arrowhead points to the area of sub-bone fracture/destruction filled with fibrocartilage-like tissue; open arrowheads point to the surface of exposed sub-bone with sclerosis. G0 = no sub-bone changes, G1 = sub-bone grade 1, G2 = sub-bone grade 2, G3 = sub-bone grade 3. Safranin-O and fast green stains, counterstained with hematoxylin. Scale bar = 100  $\mu$ m.

### 2.3.4 | Subchondral bone change

Subchondral bone plays an integral role in cartilage support and is a key component of OA pathophysiology,<sup>32</sup> but only recently has a histological subchondral bone grading in human knee joints been proposed.<sup>33</sup> The histologic subchondral bone scoring method recommended by the OARSI Initiative<sup>7</sup> for murine knee OA are: 0 = normal, 1 = mild, 2 = moderate, and 3 = severe changes. Additional subchondral bone scoring in OA mice has been described using a modified Mankin score and reported in relation to the overlying articular cartilage (0–2),<sup>34</sup> which can be problematic if concomitant cartilage loss is present. Subchondral bone changes in guinea pig and mouse models have been quantified with either quantitative micro-CT measurement,<sup>8,35,36</sup> or with histologic slides using computer histomorphometry software.<sup>10</sup> These quantitative measurements of subchondral bone are more reliable than visual grading but are unsuitable for quick screening of the subchondral bone changes in numerous joints due to the time-consuming nature and high cost.

In the proposed new system, subchondral bone was graded as 0–3 per quadrant. Grade 0 = no subchondral thickening, Grade 1 = focalized ( $\leq 50\%$  of articular surface width) subchondral bone thickening, Grade 2 = extensive ( $> 50\%$  of articular surface width) subchondral bone thickening, Grade 3 = subchondral bone thickening with bone plate destruction, bone cyst, and/or chondrogenesis. More detailed grading criteria are presented in Table 1 and Figure 2B).

### 2.3.5 | Synovitis

The involvement of synovial inflammation in rheumatoid arthritis is well known, but low-grade synovitis also plays a role in OA pathogenesis.<sup>37,38</sup> A histological grading system for human synovitis<sup>6</sup> was also applied to mouse PTOA models.<sup>39</sup> A similar synovitis grading system, which scores synovitis based mainly on the number of lining cell layers, was reported by the OARSI for rats and guinea pigs.<sup>8,9</sup> The OARSI Initiative recommendations for grading synovitis in mice are: 0 = normal, 1 = mild, 2 = moderate, and 3 = severe changes.<sup>7</sup> Our extensive histopathologic observations on arthritis revealed that multiple layers of the synovial lining cells can be easily identified in human OA, but not in murine OA models even at high magnifications. Therefore, it would be more doable to use the overall thickness of synovial lining and subsynovial tissue for murine synovitis scoring (Figure 3).

Synovitis was graded as 0, 1, 2, and 3 in our new grading scheme for a complete evaluation of various locations of the joint. Grade 0 represents no evidence of synovitis; Grade 1 demonstrates focalized synovial thickening including both synovial lining (intima) and subintimal (subsynovial) tissue that can be observed at either the side synovial plica (fold) adjacent to the joint capsule or the femoral intercondylar notch and tibial intercondylar eminence; Grade 2 represents extensive synovial thickening at either the side synovial plica or intercondylar notch/intercondylar eminence; and Grade 3 demonstrates extensive synovial thickening that can be observed in both the side and intercondylar areas (Figure 3 and

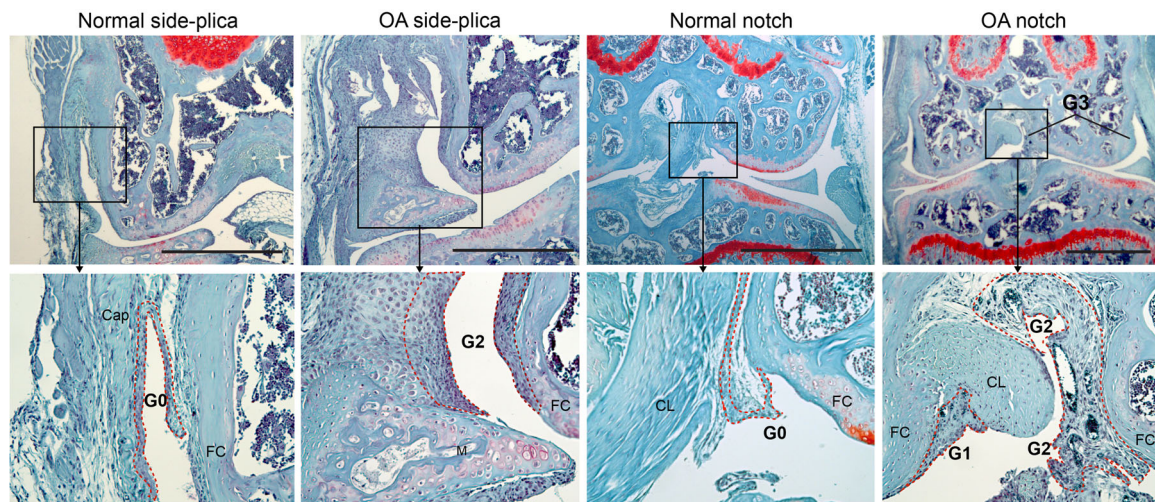


**FIGURE 3** Photomicrographs showing different grades of synovitis at low (upper panels) and higher (lower panels) magnifications. Normal side-plica graphs show normal synovium (grade 0/G0) containing synovial lining cells and thin subintimal connective tissue (outlined by a dotted orange line). OA side-plica graphs show extensive synovial thickening (grade 2/G2) in the side synovial plica around the femoral condyle (FC) and the meniscus (M). Normal notch graphs display normal synovium (grade 0/G0) containing synovial lining cells and thin subintimal connective tissue (outlined by a dotted orange line). OA notch graphs show extensive synovial thickening in both the femoral intercondylar notch (Notch) and the side synovial plica (G3, upper panel) and thickened synovium with proliferating cells and blood vessels in the subintimal connective tissue (outlined by dotted orange lines, lower panel). Safranin-O and fast green stains, counterstained with hematoxylin. CL, cruciate ligament; OA, osteoarthritis. Scale bar = 100  $\mu$ m.

Table 1). This grading method highlights the presence of low-grade synovitis in OA joints in various anatomic locations, while removing the need for time-consuming cellular analysis and cell-layer counting.

### 2.3.6 | Ectopic chondrogenesis and ossification in periarticular soft tissues

Calcification or ossification of cartilage and periarticular structures limits joint movement and has been described as one of the osteoarthritic characteristics in humans.<sup>40,41</sup> Ectopic chondrogenesis with endochondral ossification has also been demonstrated in ACLT-induced mouse models of PTOA.<sup>23</sup> Close evaluation of mouse OA models used in our laboratory further demonstrated periarticular chondrogenesis and ossification in the joint capsule as well as surrounding ligament and musculature, distinct from chondro-osteophyte formation at the joint margins. These histologic changes have not been included in any existing grading systems.

Ectopic chondrogenesis with or without ossification in the periarticular soft tissues was included in the new grading scheme. Grade 0 is normal; Grade 1 represents ectopic chondrogenesis (cartilage formation) in the synovium and capsule without ossification; Grade 2 demonstrates ectopic chondrogenesis and/or ossification in the synovium and capsule; Grade 3 has all Grade 2 changes extending into the surrounding ligament and/or musculature (Figure 4 and Table 1).

### 2.3.7 | Terminology of the new OA scoring system

Anatomic term: Knee (femorotibial) joint = stifle joint (for veterinary science).

Maximum score: Proposed scores/grades for cartilage (0–7), osteophytes (0–3), subchondral bone (0–3), synovitis (0–3), ectopic endochondral ossification (0–3) were set for each quadrant: medial femoral condyle (MFC), medial tibial plateau (MTP), lateral femoral condyle (LFC), and lateral tibial plateau (LTP) of the knee joint. This resulted in a proposed maximum score per quadrant at 19 and maximum score per joint at 76 (Table 1).

Quadrant OA score and whole-joint OA score: Quadrant OA score is referred to as an actual OA score or an averaged OA score for a quadrant of the knee joint from multiple observers. Whole-joint OA score (or joint OA score) is referred to as a total/summed score for the entire joint, including scores from all four quadrants. Scores also can be reported as or converted to an average of anatomic location subsets (e.g., MFC and MTP quadrants) or tissue subsets (e.g., cartilage, synovium, and subchondral bone, etc.) from multiple joints/images for statistical analysis.

## 2.4 | Semi-quantitative histologic OA scoring

Fifty representative tissue histologic images taken from a midcoronal section of 50 mouse knee joints were utilized for semi-quantitative scoring to test the reproducibility and sensitivity of the proposed new OA scoring scheme. Midcoronal sections

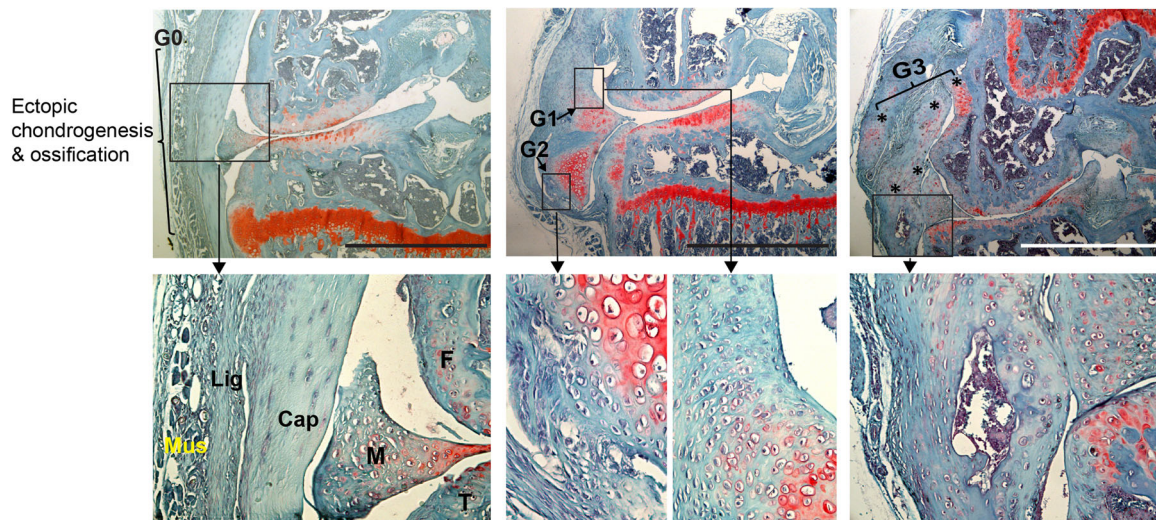


**FIGURE 4** Photomicrographs showing normal periarticular soft tissues (G0) or ectopic periarticular soft-tissue chondrogenesis (stained in red) and endochondral ossification (G1–G3). Upper panels show changes of articular cartilage and periarticular tissues in the medial compartment of the knee at low magnifications. Lower panels are magnified images of the boxes outlined in the upper panels. Left panels (G0): No ectopic chondrogenesis or ossification. Mus = muscle, Lig = ligament, Cap = capsule, M = meniscus, F = femur, T = tibia. Middle panels (G1–G2): Ectopic chondrogenic differentiation and chondrogenesis (G1) in the capsule of the medial femoral condyle quadrant and endochondral ossification (G2) limited in the synovium-capsule of the medial tibial plateau quadrant. Right panels (G3): Ectopic periarticular endochondral ossification (\*) is seen in the synovium-capsule, ligament, and musculature. Note, newly formed bone marrow cavities are seen in the ectopic ossification area. Safranin-O and fast green stains, counterstained with hematoxylin. Scale bar = 100  $\mu$ m.

were used for scoring in this study because previous studies from the authors and others have confirmed that osteoarthritic changes are more severe in the weight-bearing area (mid-portion) of rodent knee joints<sup>7,10</sup> and that a single midcoronal section can consistently define OA severity in mice.<sup>11</sup> To assess the OA severity of both cartilaginous and periarticular tissues, all the images for scoring had all knee structures covering articular cartilage, subchondral bone, joint margin, synovium, joint capsule, and surrounding ligament and musculature. The OA severity was semi-quantitatively scored by three independent observers (scorers), including an experienced observer (J.W., Observer a), a well-trained observer (C.W.G., Observer b), and a novice observer (M.J.M., Observer c) who was familiar with knee structures but had no previous experience in knee OA histopathology. A set of 25 images from 25 knees were scored twice one week apart to assess intraobserver variability from the same observer. All three observers were blinded to the information on animal groups and time points to ensure unbiased assessments.

## 2.5 | Statistics

Quantitative data were presented as means with 95% confidence intervals using JMP Pro 16 software. The significance of the difference between means from two groups was analyzed by Student's *t*-test; the difference between means for three or more groups was assessed by one-way ANOVA, followed by a post hoc

test (Tukey) using JMP Pro software. Pearson's correlation coefficient analysis and variance assumptions of specific statistical approaches were conducted using R software: A Language and Environment for Statistical Computing, Version 4.0.3. The sample size calculations were based on our preliminary data, which indicated that 6 mice per strain/time point would provide 80% power ( $\alpha = 0.05$ ,  $\beta = 0.2$ , effect size = 2.00) to detect statistical differences between the experimental groups. A *p* value of less than 0.05 was considered statistically significant.

## 3 | RESULTS

### 3.1 | Validation of inter- and intraobserver reproducibility

Histologic images from 25 midcoronal knee sections derived from 25 mice with various degrees of spontaneous or posttraumatic OA pathology were utilized for inter- and intraobserver correlation coefficient analysis to validate the reproducibility of the new grading scheme. The results demonstrated high reproducibility with interobserver correlation coefficients of  $>0.96$  for both the first and second measurement of the whole-joint scores across the experienced, trained, and novice observers (Figure 5A). Intraobserver variability analysis of the same set of histologic images also showed high reproducibility between the first and second measurement scores for each of the three observers with an

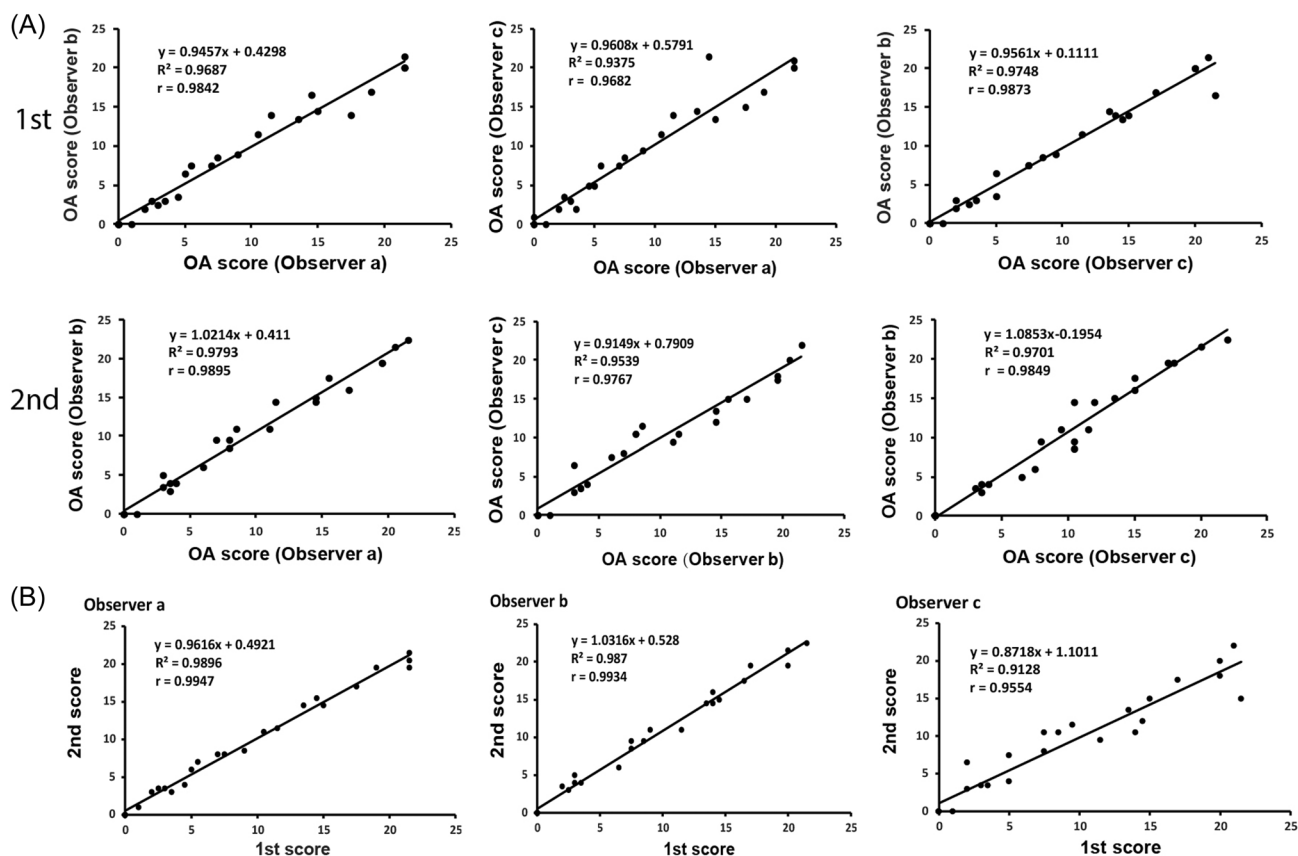


**FIGURE 5** Inter- and intraobserver variation tests with correlation coefficient values showing high reproducibility across experienced and novice observers. (A) Interobserver variability analysis of the first (1st) and second (2nd) measurement scores between the experienced (observer a), trained (observer b), and novice (observer c). (B) Intraobserver variability analysis of the first and second measurement scores for each of the three observers.  $N = 25$  for both (A) and (B).

intraobserver correlation coefficient ( $r$  value) of 0.99, 0.99, and 0.95 for experienced, trained, and novice observers, respectively (Figure 5B).

Additional six midcoronal histologic images from six separate mice with posttraumatic knee OA at 16 weeks post-DMM surgery were scored to validate the reproducibility of the new grading scheme at both the whole-joint and tissue-specific levels. Student's  $t$ -tests and ANOVA analysis showed no significant differences in the mean of OA scores between the observers (Figure 6A,B). Another set of seven midcoronal histologic images from 7 *Nfat1*<sup>-/-</sup> mice with spontaneous knee OA at the age of 24 months were also scored at both the whole-joint and tissue-specific levels (Figure 6C,D). Statistical analyses revealed no significant differences in the mean of OA scores between the observers, although minor score discrepancies between the observers were seen on some images (Figure 6A,D).

### 3.2 | Validation of sensitivity and reliability

To test the sensitivity of the new OA grading scheme, averaged whole-joint OA scores at 2 and 4 weeks post-DMM ( $n = 6$  per time

point) were determined by each of the three observers and compared statistically. The data demonstrated that the new grading scheme was able to detect minimal but significant OA progression from 2 to 4 weeks post-DMM (Figure 7A).

To test the reliability or accuracy of the new grading scheme, averaged quadrant OA scores for images of knee OA at 16 weeks post-DMM surgery were determined by each of the three observers using the same images for Figure 6A,B and analyzed statistically. The data demonstrated the most severe OA lesions in the MTP quadrant (Figure 7B), consistent with our general histopathologic findings and the reports from others.<sup>10,23</sup>

## 4 | DISCUSSION

Although several histologic OA grading systems have been reported for humans and various species of animal models,<sup>3–11</sup> the widely used OARSI Initiative system for mouse knee OA mainly focuses on cartilage lesions with subjective grading (e.g., mild, moderate, and severe) for osteophytes, subchondral bone thickening, and synovitis.<sup>7</sup> The present study has developed a new comprehensive and reproducible grading scheme for mouse knee

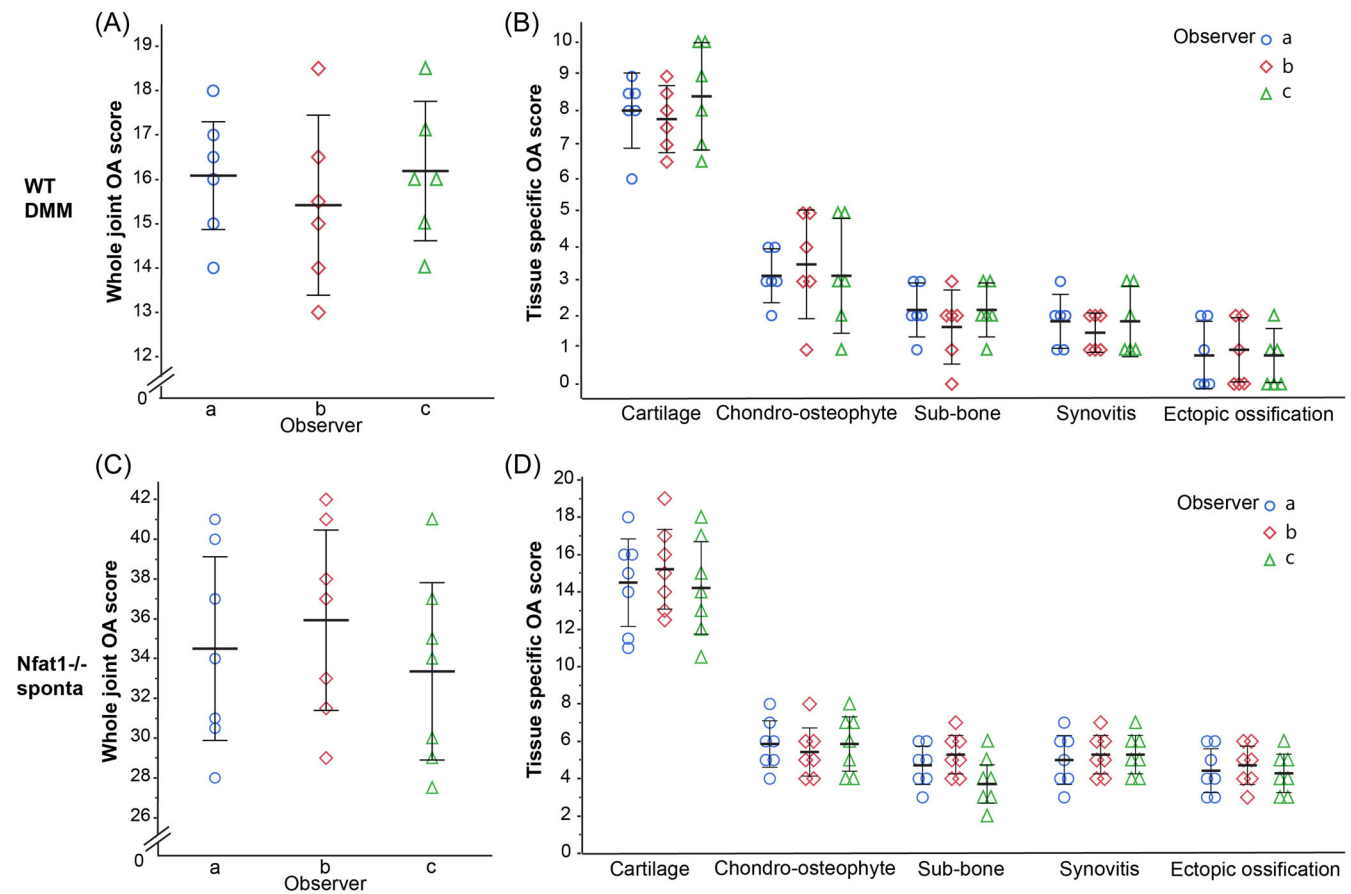


**FIGURE 6** Column scatter plots with individual data points showing variability analyses of whole-joint and tissue-specific OA scores between the three observers. (A) Whole-joint OA scores of DMM-induced posttraumatic knee OA in wild-type (WT DMM) mice demonstrate no significant difference in OA score between the observers. (B) Tissue-specific scoring of the images used for (A) shows no significant difference in OA score between the observers on any tissues/changes.  $N = 6$  for both (A) and (B). (C) Whole-joint OA scores of spontaneous knee OA in  $Nfat1^{-/-}$  mice ( $Nfat1^{-/-}$  sponta) demonstrate no significant difference between the observers. (D) Tissue-specific scoring of the images used for (C) shows no significant difference in OA score between the observers.  $N = 7$  for both (C) and (D). Ectopic ossification = Ectopic chondrogenesis and endochondral ossification in periarticular soft tissues. The short horizontal lines and corresponding error bars within the data points represent mean values and 95% confidence intervals for all four charts. DMM, destabilization of the medial meniscus; OA, osteoarthritis.

OA, which contains specific OA grading criteria for both articular cartilage and periarticular tissues as described in Table 1. Its inter- and intraobserver reproducibility as well as sensitivity and reliability have been rigorously validated. The novelty, significance, application, and possible limitations of the new scheme are discussed below.

The most prominent contribution of the new scheme is to include a grading category of ectopic ossification in the periarticular soft tissues. Ossification or calcification in the periarticular soft tissues is an important osteoarthritic feature in humans<sup>40,41</sup> and mice<sup>19,23</sup> but has not been included so far in any of the existing OA grading systems. Our studies have revealed that periarticular soft-tissue ossification begins with metaplastic chondrogenic differentiation of fibroblast-like mesenchymal cells in the synovium, joint capsule, periarticular ligament, and musculature, followed by the endochondral sequence of ossification. These histopathologic

changes are remarkable with high grades in the knee joints of  $Nfat1^{-/-}$  mice at 24 months of age and are less severe in WT mice with DMM after 16 weeks of surgery (Figure 6), but are uncommon in the earlier phase of DMM-induced knee OA (2–8 weeks post-surgery). Since OA is a disease of the entire joint, it is essential to include the periarticular soft-tissue changes in the whole-joint grading scheme.

To enhance the sensitivity for detecting early OA changes, the new scheme has included the following scoring elements: cartilage grade 1.5 to highlight the loss of surface lamina, an important histopathologic feature of early OA progression; chondro-osteophyte grade 1 to identify chondrophytes, the early phase of osteophyte formation; focalized subchondral bone thickening; focalized synovial thickening; as well as ectopic chondrogenesis in the synovium and joint capsule. The new scoring system is confirmed to be very sensitive to early OA

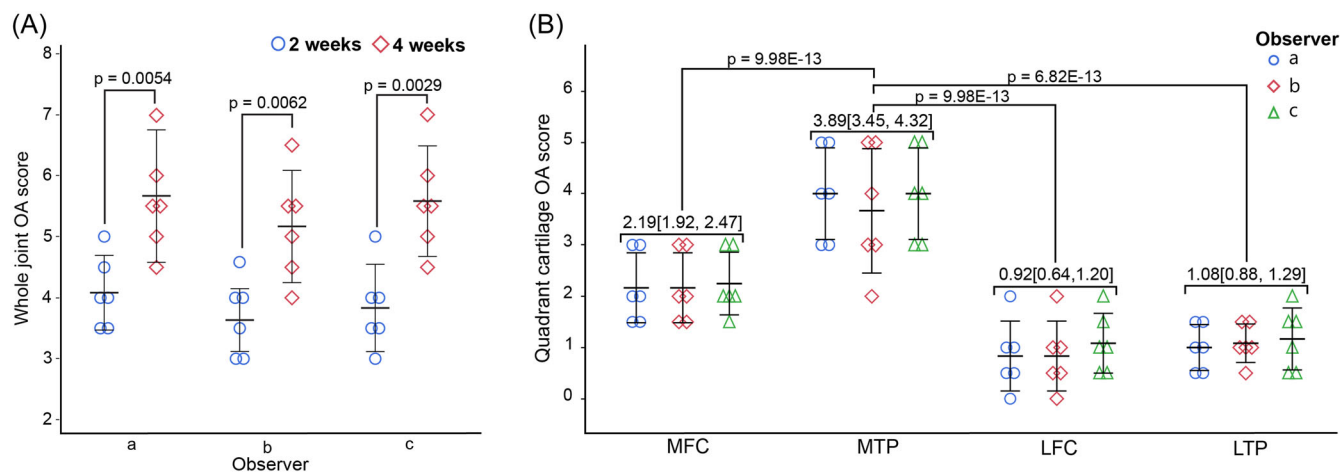


**FIGURE 7** Averaged whole-joint scores and quadrant cartilage scores showing high sensitivity and reliability of the new OA grading scheme. (A) Averaged whole-joint OA scores (from all joint tissues of WT knees) at 2 and 4 weeks post-DMM demonstrate that the new scheme can detect minimal but significant OA progression from 2 to 4 weeks post-DMM.  $N = 6$  per timepoint for each observer. (B) Averaged quadrant cartilage OA scores from each observer at 16 weeks post-DMM indicate more severe OA in the MTP quadrant than MFC, LFC, and LTP quadrants.  $N = 6$ . The numerical numbers above the scatter data points represent the mean (95% confidence interval) from three observers for each anatomic region. DMM, destabilization of the medial meniscus; OA, osteoarthritis.

changes and minor disease progression, which is essential for evaluating in vivo efficacy of OA therapies.

This new scheme more clearly defines scoring criteria for the periarticular changes (Table 1), compared to the OARSI Initiative for mouse knee OA<sup>7</sup> that grades osteophytes, subchondral bone change, and synovitis as 0–3 for normal, mild, moderate, and severe changes, respectively. Additionally, the new scheme has included two new grades for loss of cartilage with exposure of the subchondral bone (cartilage grades 6–7), a new element for subchondral bone destruction/cyst formation (subchondral bone grade 3), and synovitis in the femoral intercondylar notch (synovitis grades 2–3). Those changes were frequently seen in mouse models of OA.

The proposed grading system looking at essentially all joint tissues has multiple advantages: First, understanding the changes in surrounding joint tissues can further elucidate tissue-specific pathogenic mechanisms of OA. Second, detecting early changes in various joint tissues before cartilage destruction may identify modifiable factors that can be targeted to slow OA progression. Third, identifying OA models that have a higher propensity for tissue-specific changes will further classify the histopathologic features of individual OA models.

The knee OA grading scheme presented here can be used for evaluating in vivo efficacy assessment of various OA therapies, as it fulfills the principles of an ideal OA grading system including simplicity, utility, scalability, extensibility, and comparability as defined by the OARSI working group.<sup>5</sup> This new grading scheme is suitable not only for mild and moderate OA, but also for severe OA seen in late-stage spontaneous and posttraumatic knee OA. The simple but relatively objective new scoring elements will allow facile scoring of histologic images without using additional analytic tools such as histomorphometric software and/or micro-CT,<sup>10,42–46</sup> which are not particularly suitable for rapid assessment of numerous histologic images of knee OA involving multiple joint tissues.

Although the scheme was developed using specific mouse knee OA models, we believe that this new scoring scheme could be generalizable to other rodent models of knee OA.

The new scheme may have some limitations. First, the semi-quantitative scoring elements may allow for some subjectivity and variability in grading. Although statistical analyses have revealed high reproducibility of this scheme with no significant differences in the mean score between the observers, minor score discrepancies among the observers are noticed on some images as expected. Therefore, it is essential to use averaged score values from multiple observers for final data analyses. Second, like most of the existing knee OA grading systems, this scheme does not include the meniscus because meniscal injury is the initial cause of DMM-induced knee OA. If a grading scheme is designed solely for spontaneous OA, a meniscus grading category could be easily added. Third, OA may develop at a young age in mouse models which may have a different ratio of subchondral bone to articular cartilage and a higher incidence of periarticular soft tissue ossification, when compared to human patients with OA. Finally, comparative studies are needed to validate whether this new methodology would result in superior assessments of OA mouse models over the existing grading systems. Despite those possible limitations, the distinct advantages of this whole-joint OA grading scheme would be well-recognized and well-accepted by the research community after comparative studies and extensive scientific communications among the OA researchers and professional societies for musculoskeletal disorders.

In conclusion, the current study presents a newly developed histopathologic grading scheme for murine knee OA, which is modified from but may overcome many important weaknesses or limitations of the existing grading systems. This whole-joint grading scheme covers all-stage osteoarthritic changes in all major joint tissues, enabling us to score OA severity for the entire femorotibial

joint with high intra- and interobserver reproducibility across experienced and novice scorers. It can detect minimal but significant OA progression between two time points within a short interval. This new scheme may serve as an additional option for murine knee OA grading, particularly for rapid assessments of whole-joint OA severity for numerous histologic images.

#### AUTHOR CONTRIBUTIONS

**Caleb W. Grote, Matthew J. Mackay, and Jinxi Wang:** Literature search, data acquisition and interpretation, and manuscript preparation. **Qinghua Lu:** Histologic analysis and selection of representative histologic images. **Xiangliang Liu:** Statistical analysis and graphic preparation. **Anders R. Meyer (Pathologist):** Histopathologic analysis of grading criteria and diagnostic confirmation of synovitis. All authors have critically revised the intellectual content and approved the final manuscript for submission.

#### ACKNOWLEDGMENTS

The original breeders of *Nfat1*<sup>-/-</sup> mice used in this study were a kind gift from Dr. Laurie Glimcher (Harvard School of Public Health). Some aged wild-type mice used in this study were gifted from the National Institute on Aging (NIA). This work was supported by the National Institutes of Health (NIH) under Award number R01 AR059088 (to JW), the Department of Defense (DOD) Peer Reviewed Medical Research Program under Award number W81XWH-12-1-0304 (to JW), and The Mary & Paul Harrington Distinguished Professorship Endowment.

#### CONFLICT OF INTEREST

The authors declare no conflict of interest.

#### ORCID

Jinxi Wang  <http://orcid.org/0000-0002-8626-5637>

#### REFERENCES

- Kotlarz H, Gunnarsson CL, Fang H, Rizzo JA. Insurer and out-of-pocket costs of osteoarthritis in the US: evidence from national survey data. *Arthritis Rheum.* 2009;60:3546-3553.
- Aigner T, Cook JL, Gerwin N, et al. Histopathology atlas of animal model systems-overview of guiding principles. *Osteoarthr Cartil.* 2010;18(Suppl 3):S2-S6.
- Mankin HJ, Dorfman H, Lippiello L, Zarins A. Biochemical and metabolic abnormalities in articular cartilage from osteo-arthritic human hips. II. Correlation of morphology with biochemical and metabolic data. *J Bone Jt Surg.* 1971;53:523-537.
- Chambers MG, Cox L, Chong L, et al. Matrix metalloproteinases and aggrecanases cleave aggrecan in different zones of normal cartilage but colocalize in the development of osteoarthritic lesions in STR/ort mice. *Arthritis Rheum.* 2001;44:1455-1465.
- Pritzker KPH, Gay S, Jimenez SA, et al. Osteoarthritis cartilage histopathology: grading and staging. *Osteoarthr Cartil.* 2006;14:13-29.
- Krenn V, Morawietz L, Burmester GR, et al. Synovitis score: discrimination between chronic low-grade and high-grade synovitis. *Histopathology.* 2006;49:358-364.
- Glasson SS, Chambers MG, Van Den Berg WB, Little CB. The OARSI histopathology initiative - recommendations for histological assessments of osteoarthritis in the mouse. *Osteoarthr Cartil.* 2010;18(Suppl 3):S17-S23.
- Kraus VB, Huebner JL, DeGroot J, Bendele A. The OARSI histopathology initiative - recommendations for histological assessments of osteoarthritis in the guinea pig. *Osteoarthr Cartil.* 2010;18(Suppl 3):S35-S52.
- Gerwin N, Bendele AM, Glasson S, Carlson CS. The OARSI histopathology initiative-recommendations for histological assessments of osteoarthritis in the rat. *Osteoarthr Cartil.* 2010;18(Suppl 3):S24-S34.
- McNulty MA, Loeser RF, Davey C, Callahan MF, Ferguson CM, Carlson CS. A comprehensive histological assessment of osteoarthritis lesions in mice. *Cartilage.* 2011;2:354-363.
- Armstrong AR, Carlson CS, Rendahl AK, Loeser RF. Optimization of histologic grading schemes in spontaneous and surgically-induced murine models of osteoarthritis. *Osteoarthr Cartil.* 2021;29:536-546.
- Loeser RF, Goldring SR, Scanzello CR, Goldring MB. Osteoarthritis: a disease of the joint as an organ. *Arthritis Rheum.* 2012;64:1697-1707.
- Goldring MB, Goldring SR. Osteoarthritis. *J Cell Physiol.* 2007;213:626-634.
- McCoy AM. Animal models of osteoarthritis: comparisons and key considerations. *Vet Pathol.* 2015;52:803-818.
- Lorenz J, Grassel S. Experimental osteoarthritis models in mice. *Methods Mol Biol.* 2014;1194:401-419.
- Fang H, Beier F. Mouse models of osteoarthritis: modelling risk factors and assessing outcomes. *Nat Rev Rheumatol.* 2014;10:413-421.
- Xanthoudakis S, Viola JPB, Shaw KTY, et al. An enhanced immune response in mice lacking the transcription factor NFAT1. *Science.* 1996;272:892-895.
- Hodge MR, Ranger AM, de la Brousse FC, Hoey T, Grusby MJ, Glimcher LH. Hyperproliferation and dysregulation of IL-4 expression in NF-ATp-deficient mice. *Immunity.* 1996;4:397-405.
- Wang J, Gardner BM, Lu Q, et al. Transcription factor *Nfat1* deficiency causes osteoarthritis through dysfunction of adult articular chondrocytes. *J Pathol.* 2009;219:163-172.
- Zhang M, Lu Q, Egan B, Zhong X, Brandt K, Wang J. Epigenetically mediated spontaneous reduction of NFAT1 expression causes imbalanced metabolic activities of articular chondrocytes in aged mice. *Osteoarthr Cartil.* 2016;24:1274-1283.
- Zhang M, Lu Q, Budden T, Wang J. NFAT1 protects articular cartilage against osteoarthritic degradation by directly regulating transcription of specific anabolic and catabolic genes. *Bone Jt Res.* 2019;8:90-100.
- Rodova M, Lu Q, Li Y, et al. *Nfat1* regulates adult articular chondrocyte function through its age-dependent expression mediated by epigenetic histone methylation. *J Bone Miner Res.* 2011;26:1974-1986.
- Glasson SS, Blanchet TJ, Morris EA. The surgical destabilization of the medial meniscus (DMM) model of osteoarthritis in the 129/SvEv mouse. *Osteoarthr Cartil.* 2007;15:1061-1069.
- Collins DH, McElligott TF. Sulphate (35SO<sub>4</sub>) uptake by chondrocytes in relation to histological changes in osteoarthritic human articular cartilage. *Ann Rheum Dis.* 1960;19:318-330.
- Ostergaard K, Petersen J, Andersen CB, Bendtzen K, Salter DM. Histologic/histochemical grading system for osteoarthritic articular cartilage: reproducibility and validity. *Arthritis Rheum.* 1997;40:1766-1771.
- Jackson MT, Moradi B, Zaki S, et al. Depletion of protease-activated receptor 2 but not protease-activated receptor 1 may confer protection against osteoarthritis in mice through extracartilaginous mechanisms. *Arthritis Rheum.* 2014;66:3337-3348.
- Little CB, Barai A, Burkhardt D, et al. Matrix metalloproteinase 13-deficient mice are resistant to osteoarthritic cartilage erosion but not chondrocyte hypertrophy or osteophyte development. *Arthritis Rheum.* 2009;60:3723-3733.
- Kamekura S, Hoshi K, Shimoaka T, et al. Osteoarthritis development in novel experimental mouse models induced by knee joint instability. *Osteoarthr Cartil.* 2005;13:632-641.

29. Hayami T, Pickarski M, Zhuo Y, Wesolowski GA, Rodan GA, Duong LT. Characterization of articular cartilage and subchondral bone changes in the rat anterior cruciate ligament transection and meniscectomized models of osteoarthritis. *Bone*. 2006;38:234-243.
30. Sniekers YH, van Osch GJVM, Ederveen AGH, et al. Development of osteoarthritic features in estrogen receptor knockout mice. *Osteoarthr Cartil*. 2009;17:1356-1361.
31. Wachsmuth L, Engelke K. High-resolution imaging of osteoarthritis using microcomputed tomography. *Methods Mol Med*. 2004;101:231-248.
32. Walsh DA, McWilliams DF, Turley MJ, et al. Angiogenesis and nerve growth factor at the osteochondral junction in rheumatoid arthritis and osteoarthritis. *Rheumatology*. 2010;49:1852-1861.
33. Aho OM, Finnilä M, Thevenot J, Saarakkala S, Lehenkari P. Subchondral bone histology and grading in osteoarthritis. *PLoS One*. 2017;12:e0173726.
34. Furman BD, Strand J, Hembree WC, Ward BD, Guilak F, Olson SA. Joint degeneration following closed intraarticular fracture in the mouse knee: a model of posttraumatic arthritis. *J Orthop Res*. 2007;25:578-592.
35. Ding M, Christian Danielsen C, Hvid I. Effects of hyaluronan on three-dimensional microarchitecture of subchondral bone tissues in guinea pig primary osteoarthrosis. *Bone*. 2005;36:489-501.
36. Botter SM, van Osch GJVM, Waarsing JH, et al. Cartilage damage pattern in relation to subchondral plate thickness in a collagenase-induced model of osteoarthritis. *Osteoarthr Cartil*. 2008;16:506-514.
37. Pessler F, Dai L, Diaz-Torne C, et al. The synovitis of "non-inflammatory" orthopaedic arthropathies: a quantitative histological and immunohistochemical analysis. *Ann Rheum Dis*. 2008;67:1184-1187.
38. Benito MJ. Synovial tissue inflammation in early and late osteoarthritis. *Ann Rheum Dis*. 2005;64:1263-1267.
39. Lewis JS, Hembree WC, Furman BD, et al. Acute joint pathology and synovial inflammation is associated with increased intra-articular fracture severity in the mouse knee. *Osteoarthr Cartil*. 2011;19:864-873.
40. Ea HK, Nguyen C, Bazin D, et al. Articular cartilage calcification in osteoarthritis: insights into crystal-induced stress. *Arthritis Rheum*. 2011;63:10-18.
41. Hubert J, Hawellek T, Moe M, et al. Labral calcification in end-stage osteoarthritis of the hip correlates with pain and clinical function. *J Orthop Res Off Publ Orthop Res Soc*. 2018;36:1248-1255.
42. Ruan MZC, Patel RM, Dawson BC, Jiang MM, Lee BHL. Pain, motor and gait assessment of murine osteoarthritis in a cruciate ligament transection model. *Osteoarthr Cartil*. 2013;21:1355-1364.
43. Staines KA, Ikpegbu E, Törnqvist AE, et al. Conditional deletion of E11/podoplanin in bone protects against load-induced osteoarthritis. *BMC Musculoskelet Disord*. 2019;20:344.
44. Cai A, Hutchison E, Hudson J, et al. Metabolic enrichment of omega-3 polyunsaturated fatty acids does not reduce the onset of idiopathic knee osteoarthritis in mice. *Osteoarthr Cartil*. 2014;22:1301-1309.
45. Bendele AM, Hulman JF. Effects of body weight restriction on the development and progression of spontaneous osteoarthritis in guinea pigs. *Arthritis Rheum*. 1991;34:1180-1184.
46. Sampson ER, Beck CA, Ketz J, et al. Establishment of an index with increased sensitivity for assessing murine arthritis. *J Orthop Res*. 2011;29:1145-1151.

#### SUPPORTING INFORMATION

Additional supporting information can be found online in the Supporting Information section at the end of this article.

**How to cite this article:** Grote CW, Mackay MJ, Lu Q, Liu X, Meyer AR, Wang J. A Whole-Joint histopathologic grading system for murine knee osteoarthritis. *J Orthop Res*. 2023;41:1407-1418. doi:10.1002/jor.25482